Variable Conductance Heat Pipes for Radioisotope Stirling Systems

William G. Anderson and Calin Tarau

Advanced Cooling Technologies, Inc., Lancaster, PA 17601 U.S.A.
717-295-6104, Bill.Anderson@1-ACT.com

Abstract. In a Stirling radioisotope system, heat must continually be removed from the GPHS modules, to maintain the GPHS modules and surrounding insulation at acceptable temperatures. Normally, the Stirling convertor provides this cooling. If the Stirling engine stops in the current system, the insulation is designed to spoil, preventing damage to the GPHS, but also ending the mission. An alkali-metal Variable Conductance Heat Pipe (VCHP) was designed to allow multiple stops and restarts of the Stirling engine. A VCHP was designed for the Advanced Stirling Radioisotope Generator, with a 850°C heater head temperature. The VCHP turns on with a ΔT of 30°C, which is high enough to not risk standard ASRG operation but low enough to save most heater head life. This VCHP has a low mass, and low thermal losses for normal operation. In addition to the design, a proof-of-concept NaK VCHP was fabricated and tested. While NaK is normally not used in heat pipes, it has an advantage in that it is liquid at the reservoir operating temperature, while Na or K alone would freeze. The VCHP had two condensers, one simulating the heater head, and the other simulating the radiator. The experiments successfully demonstrated operation with the simulated heater head condenser off and on, while allowing the reservoir temperature to vary over 40 to 120°C, the maximum range expected. In agreement with previous NaK heat pipe tests, the evaporator ΔT was roughly 70°C, due to distillation of the NaK in the evaporator.

Keywords: Alkali metal heat pipes, variable conductance heat pipes, radioisotope Stirling systems, NaK heat pipes, Advanced Stirling Radioisotope Generator, space radiator systems.
PACS: 44.30.+v, 44.35.+c.

INTRODUCTION

In a Stirling radioisotope power system, one or more General Purpose Heat Sources (GPHSs) supply heat to a Stirling engine. This heat is used to generate electric power, and the waste heat is radiated to space. In a GPHS, the radioisotope plutonium-238 (Pu-238) used to produce the heat is encapsulated into an iridium cladding forming a fueled clad. The fueled clads are surrounded by graphite. The maximum allowable GPHS module operating temperature is set by the iridium cladding around the Pu-238 fuel. The GPHS module is designed to protect and contain the plutonium and reduce the chance of plutonium release in launch accident situations. However, if the iridium cladding is overheated, grain boundary growth can weaken the cladding, possibly increasing the chances and amounts of plutonium that could be released during an accident.

Heat must continually be removed from the GPHS modules, to maintain the GPHS modules and surrounding insulation at acceptable temperatures. Normally, the Stirling engine removes the heat, keeping the GPHS modules cool. There are three basic times when it may be desirable to stop and restart the Stirling engine: (1) During installation of the GPHS it might be desirable to stop the Stirling engine, (2) During some missions, it may be desirable to briefly stop the Stirling engine to minimize electromagnetic interference and vibration while taking scientific measurements, and (3) Without the VCHP, any unexpected stoppage of the convertor during operation on the ground or during a mission could cause the insulation to spoil to protect the GPHS. The VCHP could potentially allow convertor operation to be restarted, depending on the reason for stoppage. It would also save replacing the insulation after such an event during ground testing.

The schematics in Fig. 1a and b show the basic concept of the VCHP integrated with a Stirling engine. The evaporator of the VCHP is in contact with the GPHS module(s). The non-condensable gas (NCG) charge in the

system is sized so the secondary radiator is blocked during normal operation and the VCHP delivers heat to the heater head; see Fig. 1(a). When the Stirling engine is stopped, the temperature of the entire system starts to increase. Since the VCHP system is saturated, the working fluid vapor pressure increases as the temperature increases. This compresses the NCG. As shown in Fig. 1(b), this opens up the radiator. Once the radiator is fully open, all of the heat is dumped to the radiator, and the temperature stabilizes. Once the Stirling engine starts operating again, the vapor temperature and pressure start to drop. The non-condensable gas blankets the radiator, and the system is back to the normal state (Fig. 1(a)).

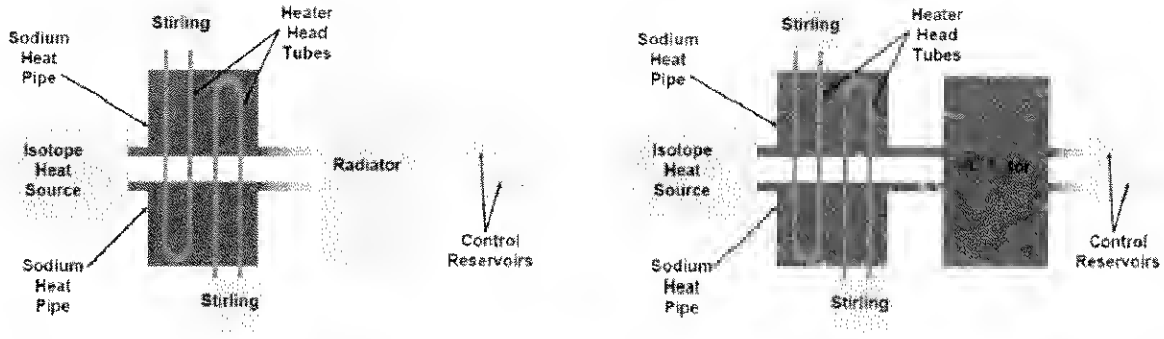

(a) Stirling engine is operating. **(b)** Stirling engine is stopped.

FIGURE 1. VCHP Dumps Waste Heat to the Radiator when the Stirling Engine is Stopped.

VCHP Requirements

The Advanced Stirling Radioisotope Generator (ASRG) (Chan, Wood, and Schreiber, 2007) was selected as the baseline design. The system consists of two Advanced Stirling Converters (ASCs), mounted back to back to minimize vibration. Heat to each ASC is supplied by one GPHS module. During operation, a heat collector is used to conduct the heat from the GPHS into the Stirling heater head, see Fig. 2(a). A cold-side adapter flange, shown in Fig. 2(b) is used to conduct the waste heat from the Stirling engine cold side to the ASRG housing. This is fabricated from copper, and serves as a structural member. The cold-end flange temperature is primarily set by the sink temperature seen by the ASRG structure (radiator), which varies from earth (including launch) environments to deep space. Its operating temperature can range from 40 to 120°C, depending on the radiation environment that the ASRG sees. This flange was selected as the best location for a cold VCHP reservoir.

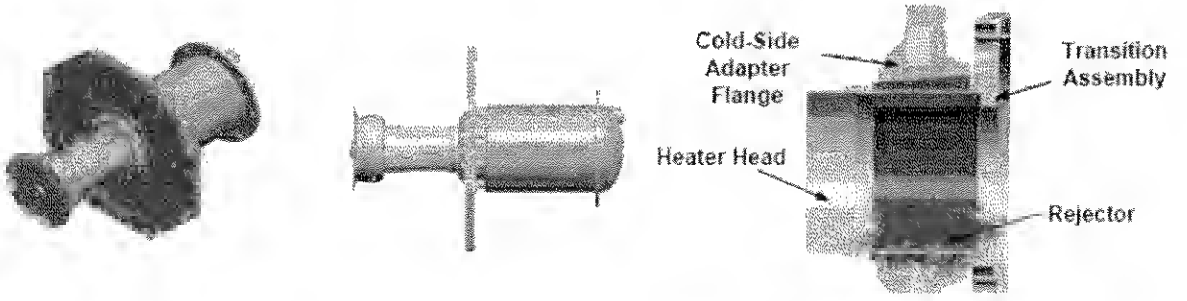

(a) Stirling Convertor with Heat Collector and Cold-Side Adapter Flange. **(b)** Cold-Side Adapter Flange.

FIGURE 2. Advanced Stirling Convertor and Cold Side Adapter Flange (taken from Chan, Wood, and Schreiber, 2007).

The heater head hot-end temperature was assumed to be 850°C for this program, compared to the current ASRG engineering unit temperature of 650°C. To accommodate this increase, the heater head material would be changed from the current Inconel 718 to Mar-M 247. Mar-M 247 is a nickel-based casting alloy designed to have good tensile and creep rupture properties at elevated temperatures.

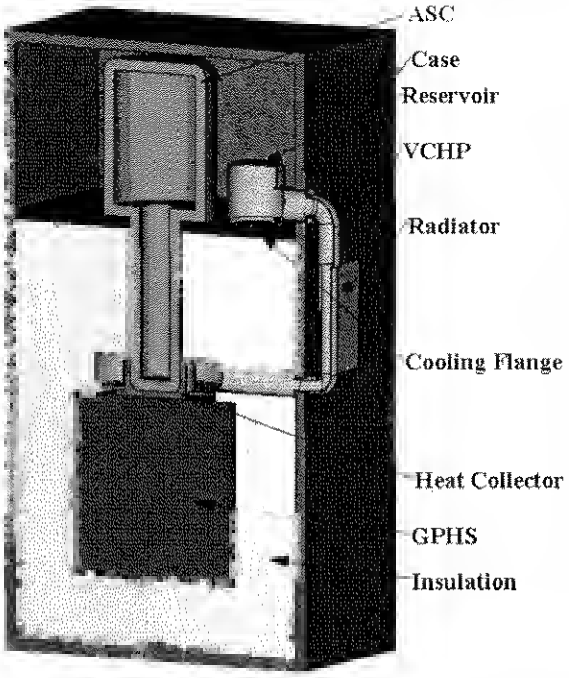

FIGURE 3. VCHP design with a non-integrated heat pipe.

INTEGRATED AND NON-INTEGRATED VCHP DESIGNS

Design requirements for the VCHP are shown in Table 1. Two related designs were examined, an integrated and a non-integrated system, see Figs. 3 and 4. In the non-integrated system, the VCHP wraps around the heat collector, while the VCHP replaces the heat collector in the integrated system. Figure 3 is a schematic of the non-integrated system. When the convertor is operating, part of the heat from the GPHS travels through the heat collector to the Stirling convertor heater head. The remainder of the heat travels through the heat pipe and then through the heat collector wall to the heater head. The radiator is blanketed by non-condensable gas. The VCHP reservoir is attached to the Cold-Side Adapter Flange. When the Stirling convertor is shut off, the temperature increases, pushing the non-condensable gas front closer to the reservoir, and dumping heat to the radiator.

The VCHP is designed to turn on completely when the heater head temperature increases to 880 °C, a ΔT of 30 °C above the normal operating temperature of 850 °C. For this preliminary design, a simple flat-front VCHP model was used (Marcus, 1972). A schematic of the non-condensable gas front location at various operating conditions is shown in Fig. 4b (it is the same for both types of heat pipe). During normal operation, the gas front is located between numbers 1 and 2 in the figure, depending on the VCHP reservoir temperature. When the reservoir is at the maximum temperature of 120 °C, the NCG pressure is high, and the front is located at 1. When the reservoir is at the minimum temperature of 40 °C, the NCG pressure is low, and the front is located at 2.

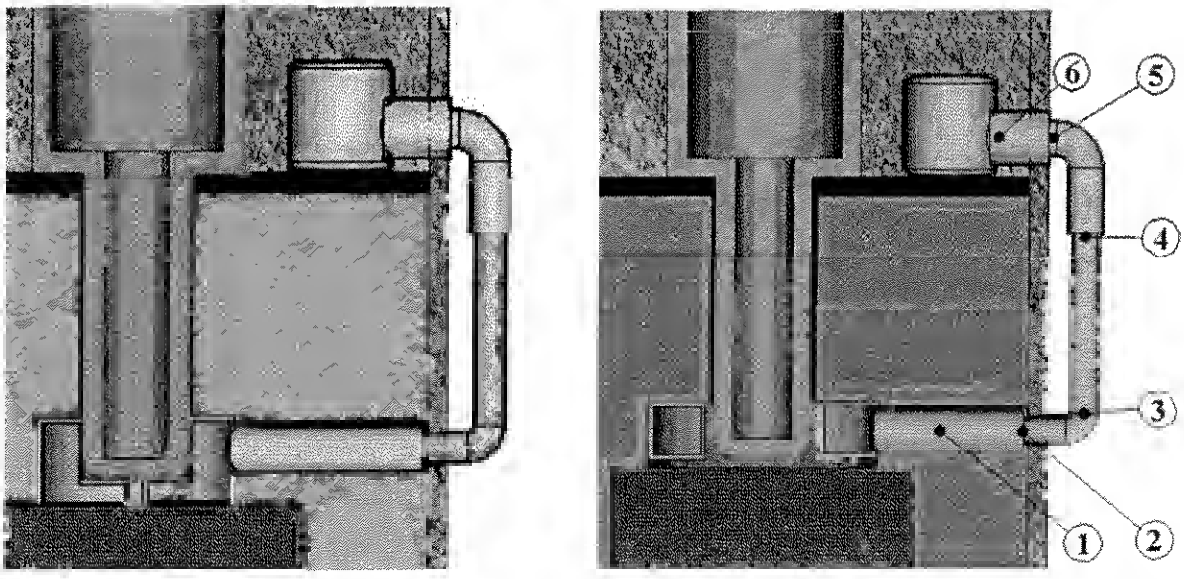

(a) Integrated VCHP.

(b) Non-Integrated VCHP.

FIGURE 4. Comparison of the Integrated and Non-Integrated Designs.

The radiator is located between numbers 3 and 4 in Fig. 4b. The design assumed a small carbon-carbon radiator. When the Stirling convertor is turned off, the temperature increases to 880 °C, and the gas front is located between numbers 4 and 5. It is at 4 for the maximum reservoir temperature, and at 5 for the minimum reservoir temperature.

The VCHP design is summarized in Table 2. The total VCHP mass is between 180 and 190 grams. The VCHP heat loss when the Stirling convertor is operational is 6.5 W. Neither the mass nor the heat loss has been optimized, and it is expected that the heat loss can be reduced.

TABLE 1. VCHP Design Requirements.

GPHS Power (W)	250
GPHS Power to the Stirling Engine (W)	225
Heater Head Temperature (°C)	850
Heater Head Material	Mar-M 247
Conduction Losses down the Heater Head Wall (W)	6.5
Heat Collector Material (Baseline)	Nickel 201
Potential Reservoir Location	Cold-Side Adapter Flange
Cold-Side Adapter Flange Temp. (°C)	40 to 120
Heat Pipe Working Fluid	Sodium or NaK
VCHP Temperature when Stirling is Off (°C)	880

TABLE 2. Summary of design parameters and material properties.

Non-conducting temperature (°C)	850
Conducting temperature (°C)	880
Reservoir minimum temperature (°C)	40
Reservoir maximum temperature (°C)	120
Sink temperature (K)	300
NCG temperature in the pipe (K)	300
Number of moles of NCG (moles)	0.0028
Radiator material	Carbon-Carbon
Radiator half length (cm)	2.8
Radiator thickness (mm)	2
Radiator height (cm)	6
Radiator emissivity	0.85
Radiator thermal conductivity (carbon-carbon) (W/m K)	300
Radiator efficiency	0.904
Heat Loss When Convertor is Operating (W)	6.5
Total mass (VCHP with reservoir and working fluid) (g)	180-190

Temperature Profiles

A summary of the results of this analysis is presented in Table 3. Here, critical/important temperatures like maximum temperature of the system (estimated GPHS temperature), average heater head wall temperature at the heat acceptor (H head Temp.), and heater head wall temperature variation along the axial length of the heat acceptor (ΔT on Path 1) are shown for all system configurations. For comparison, the heater head temperature distributions along the axial length of the heat acceptor are shown together in Fig. 5.

As shown in Table 3 and Fig. 5, adding a VCHP to the ASRG has two additional benefits. First, the heater head temperature is much more uniform, with the ΔT along the axial length of the heat acceptor decreasing from 15 °C to

3.5 – 4 °C. The Sage Stirling thermodynamic code was used to estimate the efficiency improvement gained by reducing this temperature difference (Tew, 2007). The estimated increase in power due to isothermalizing the heat acceptor is roughly 0.6 W_e. This partially offsets the power loss due to the 6.5 W additional heat loss due to the VCHP, estimated as 6.5 * 0.32 (est. convertor efficiency) = 2.1 W. This indicates that roughly one-third of the current VCHP losses will be made up by the increased Stirling convertor efficiency.

TABLE 3. Numerical Analysis Summary.

CASE	ASC ON – VCHP OFF				ASC OFF – VCHP - ON			
	ΔT on Path 1	Max Temp.	Vapor Temp.	H. head Temp.	ΔT on Path 1	Max Temp.	Vapor Temp.	H. head Temp.
No VCHP	15.5 °C	1039 °C	-	851 °C	-	-	-	-
Non-integrated VCHP	4 °C	1009 °C	856 °C	849 °C	4.2 °C	1042 °C	881 °C	882 °C
Integrated VCHP	3.5 °C	971 °C	856 °C	850 °C	1.8 °C	998 °C	881 °C	881 °C

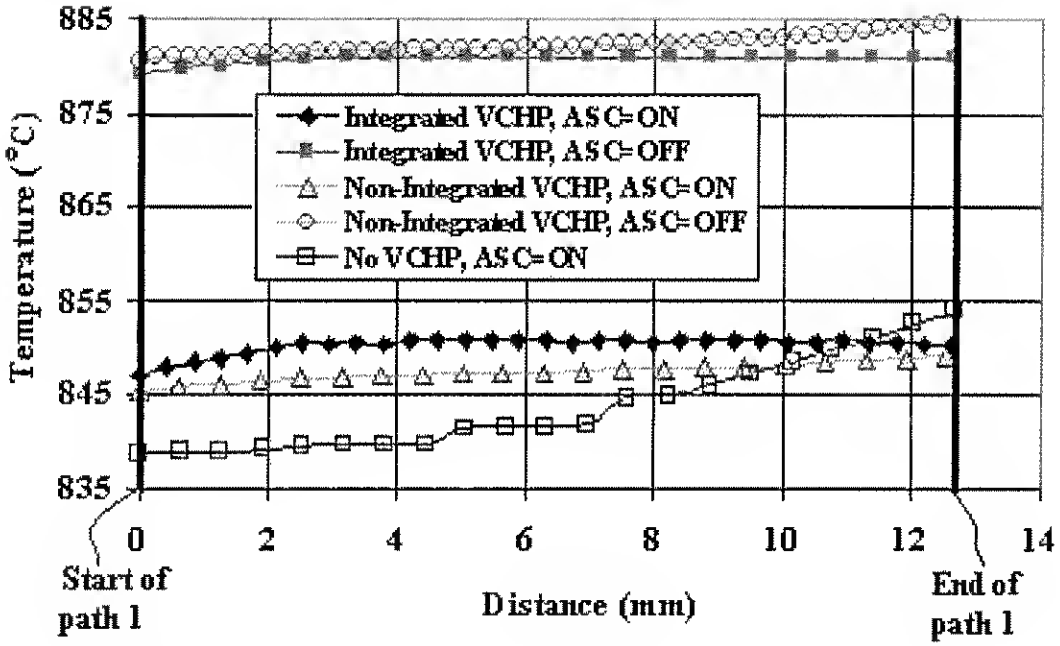

FIGURE 5. Heater Head Temperature Profiles Along the Axial Length of the Heat Acceptor for All Cases.

As shown by the estimated maximum temperature in Table 3, a second benefit is the reduction in the GPHS surface temperature. With the integrated system, most of the temperature drop occurs in the thin VCHP walls, while the evaporator vapor in the VCHP is essentially isothermal. In the non-integrated case, most of the heat is still transmitted through the VCHP rather than exclusively through the heat collector. In both cases, reducing the GPHS temperature also reduces the thermal losses though the insulation.

HEAT PIPE MATERIALS

The selection of the heat pipe envelope and working fluid is discussed below.

Heat Pipe Envelope

In the 850 °C ASRG, the heater head will be fabricated with Mar-M 247. Mar-M 247 was rejected as a candidate for the heat pipe wall material, due to the relatively high 5.5% aluminum content. Sodium and potassium are known

to attack aluminum, so we are concerned about the long-term compatibility of Mar-M with NaK in a heat pipe. Instead, the VCHP would be fabricated from either Inconel 718 or Haynes 230 in the Phase II heat pipes, since they are known to be compatible with sodium based on long duration life tests (Rosenfeld, et al, 2004). NASA Glenn conducted a life test at 700°C for 41,000 hours with sodium with an Inconel 718 envelope and a 316 stainless steel wick. NASA Glenn has also tested sodium at 700°C with a Haynes 230 envelope and a sintered nickel wick structure for 20,000 hours before the test was stopped. Neither of these tests had any problems. (Rosenfeld, et al, 2004).

Anderson, Rosenfeld, and Noble (1991) conducted a NaK pool-boiler life test with a small amount of xenon added to promote boiling. The evaporator was fabricated from Inconel 635, while the condenser was fabricated from 316 stainless steel. The evaporator had a -100+140 mesh 304L-stainless-steel wick. The system was life tested for over 800 hours at 700 °C, including multiple cold and warm restarts. Andraka et al. (1994) conducted a life test with NaK in a Haynes 230 pool boiler. The pool boiler operated for 7,500 hours, including over 1,000 start-ups from ambient. The pool boiler was operated at 750 °C around the clock, with a 1/2 hour shutdown to ambient every 8 hours. The test was terminated when a small leak developed in an Inconel 600 thermocouple well.

Heat Pipe Working Fluid

In this temperature range, there are four potential working fluids: sodium, potassium, cesium, and eutectic NaK, a mixture of sodium and potassium (roughly 78% potassium) with a low melting point. Properties at 850 °C are shown in Table 4. NaK was chosen over sodium or potassium, since it melts at -12.7 °C, significantly lower than either sodium or potassium. It will be liquid over the entire range of 40 to 120 °C for a reservoir mounted on the Cold-Side Adapter Flange. Ernst (2007) states that it is necessary to have the reservoir temperature above the melting point. During his alkali metal VCHP tests with reservoir temperatures below the freezing point, the entire fluid inventory ended up frozen in the reservoir. If sodium or potassium is used in this program, either the reservoir will have to be heated, or a different reservoir location will be required. NaK was chosen over cesium because it has a Merit number roughly 5 times higher than cesium.

TABLE 4. Sodium, Potassium, Cesium, and NaK Fluid Properties at 850 °C.

Property\Fluid	**Na**	**K**	**Cs**	**NaK**
Melting Temperature, (°C)	97.8	63.2	28.4	-12.7
Boiling Temperature, (°C)	881.4	756.5	668.4	785
Vapor Pressure, (KPa)	75.99	222.9	432.65	175.29
Surface Tension, (N/m)	0.121	0.058	0.030	0.067
Liquid Viscosity, (Pa.s)	0.000162	0.000116	0.000138	0.000129
Latent Heat, (MJ/kg)	4.41	2.05	0.50	2.57

Potential NaK Temperature Non-Uniformities

NaK is a eutectic mixture with roughly 78% potassium. Unfortunately, there is no azeotropic mixture of sodium and potassium. In an azeotropic mixture, the compositions of the liquid and vapor are identical, so the composition of the liquid does not change during boiling. In a non-azeotropic mixture, the vapor is enriched in the component with the higher vapor pressure. In the case of NaK, the vapor has a greater percentage of potassium than the liquid. In other words, if a pool of NaK was allowed to boil away (with all of the vapor removed), the fraction of sodium in the pool would continually rise. In a NaK heat pipe, the liquid is constantly replenished, so that the compositions will remain constant. However, in some cases, it is possible for temperature non-uniformities to develop, even with a constant heat flux in the evaporator (Anderson, 1993).

Figure 6 shows the dew point and bubble point curves at a constant pressure of 1 atmosphere, for liquid compositions that vary from all sodium to all potassium. The vapor pressure is 1 atm, when the temperature is 758 °C for a pool of pure liquid potassium. The temperature must be increased to 882 °C for the vapor pressure above a pure sodium pool to reach 1 atm. At all compositions in between, the vapor potassium molar fraction ("Dew Point Curve") is higher than the liquid potassium molar fraction ("Bubble Point Curve"). Eutectic NaK contains 0.675 mole fraction of potassium. As shown in Fig. 6, the temperature is 786 °C when the pressure is 1 atm. A tie line is shown in Fig. 6 between eutectic liquid NaK and its equilibrium vapor composition. Note that the vapor is enhanced in potassium when compared with the liquid, with a 0.874 mole fraction potassium.

As discussed in Anderson (1993), the variation of the liquid composition can give rise to a temperature variation. The pressure in the vapor space is constant, assume 1 atm. The liquid composition at the start of the evaporator wick will be eutectic NaK, so the vapor temperature would be 786 °C. At the end of the evaporator wick furthest from the condenser, the composition is somewhere between eutectic NaK and sodium. If we assume that the composition at the end is pure sodium, the temperature there would be 882 °C to boil off the pure sodium at the same pressure, which is almost 100 °C higher. The actual temperature variation will depend on a number of things, including how much the liquid composition changes, and how much the vapor is mixed in the evaporator.

Anderson (1993) conducted tests on a NaK heat pipe with a series of thermocouple wells to measure the temperature non-uniformities. He found that when the artery was active, uniform heat fluxes in the NaK pipe could generate 80 °C temperature non-uniformities with a 30 W/cm^2 heat flux. The temperature difference decreased to roughly 50 °C as the heat flux was increased to 53 W/cm^2, probably as a result of increased vapor mixing.

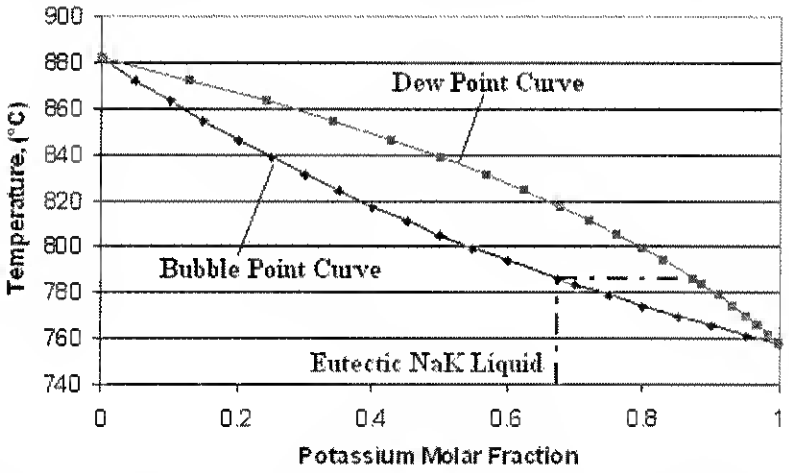

FIGURE 6. Dew point and bubble point curves for NaK vapor and liquid at a constant pressure of 0.1MPa.

Experimental NaK VCHP

The experimental VCHP was designed to demonstrate the following:

1. High temperature VCHP with NaK as the working fluid
2. Similar sizes/lengths to the Stirling application
3. Ability to operate while varying the reservoir temperature from 40 °C to 120 °C.

A schematic of the experimental VCHP is shown in Fig. 7. The pipe has a 1.91 cm (3/4") O.D., with an overall length of 60 cm. The heat pipe is a straight cylinder, with constant diameter, to minimize cost and construction time. It has the following features:

- Operate in air, with heat rejection by radiation and natural convection
- Carries about 250 W
- Heat is supplied to the evaporator with an RF coil

- NaK working fluid
- NCG: Argon (close in molecular weight to potassium)
- 304 L Stainless Steel envelope, with 304 stainless wick
- Thermocouple Wells (with long TC's to measure the evaporator temperature profile)

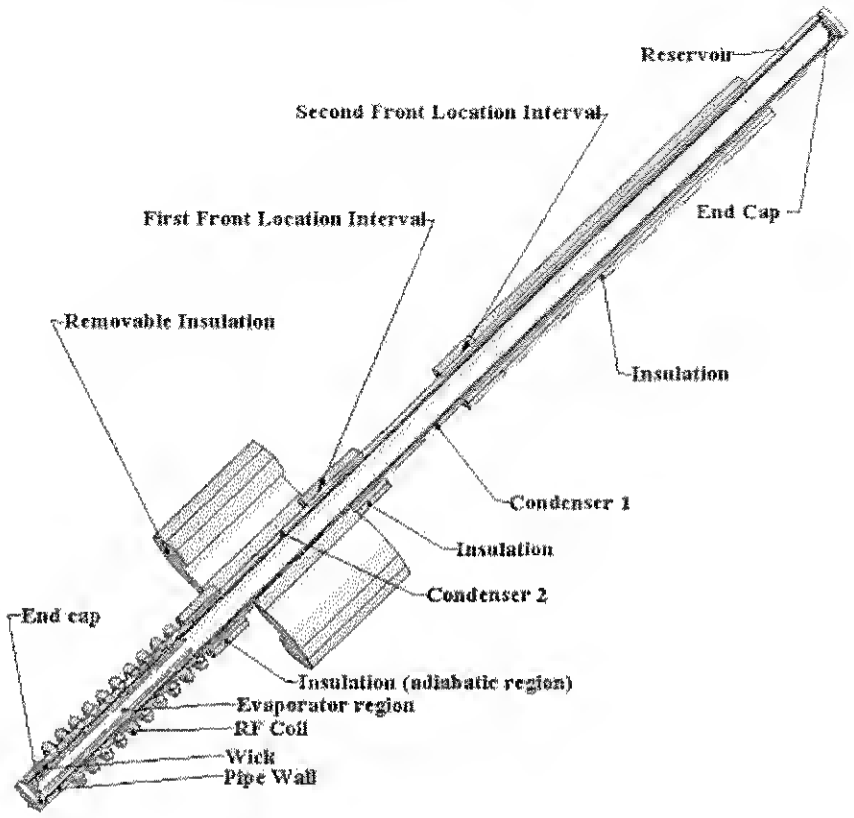

FIGURE 7. VCHP Schematic, with Condenser 2 Simulating the Stirling Engine, and Condenser 1 Simulating the Radiator.

During operation simulating when the Stirling is operating, heat is rejected from the second condenser. The VCHP was designed to operate at temperatures around 700 °C (the temperature was reduced from the ~ 850 °C heater head temperature to allow the use of inexpensive stainless steel for the heat pipe envelope).

To simulate turning the Stirling engine off, the second condenser is covered with insulation. To reject the heat, the heat pipe temperature increases and the non-condensable gas is compressed, until the vapor front passes the first condenser. Heat is then rejected from the first condenser, at a temperature roughly 30 °C higher than the original temperature. The two condensers must be on the same side of the evaporator. If the first condenser was on the other side, then some of the non-condensable gas could be trapped in the second condenser when it was blocked.

Results for a typical test with the NaK VCHP are shown in Fig. 9. Tests were conducted with the reservoir at 40 and 120 °C, the maximum and minimum reservoir temperatures. When the ASC is off, the second condenser is covered with insulation. The insulation is removed when the ASC is on. As shown in Fig. 9, the temperature increased and the front moved into the first condenser when the ASC was off.

Figure 10 shows the temperature profile in the evaporator. As expected, the temperature was highest furthest from the condenser. (See the discussion around Fig. 6). As the liquid travels through the evaporator wick, potassium is preferentially evaporated. The liquid near the end of the evaporator is mostly sodium, so the temperature increases to maintain the same vapor pressure. The ΔT should be much smaller in the ASRG VCHP, due to the smaller size and higher diffusion.

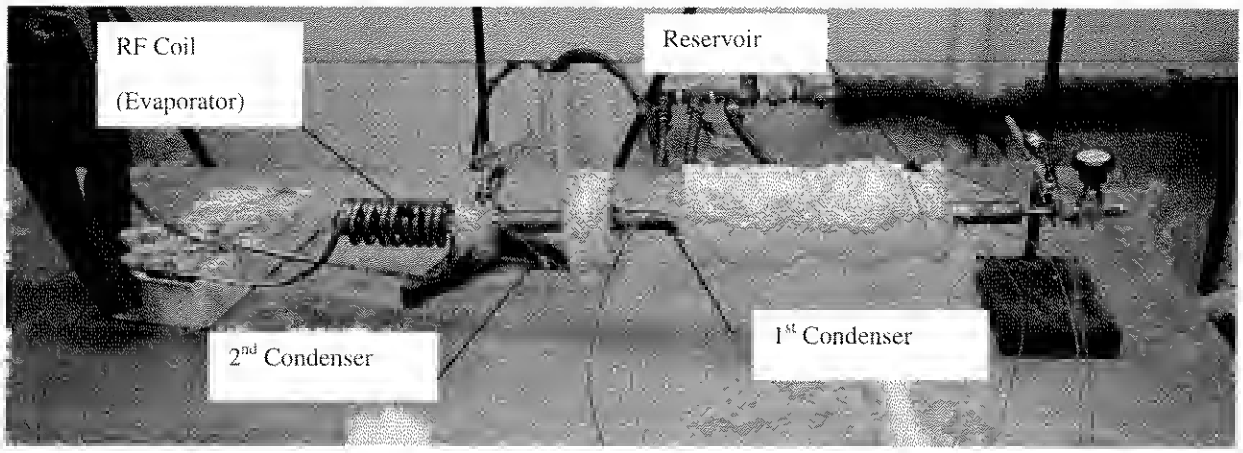

FIGURE 8. NaK VCHP Test Set-Up.

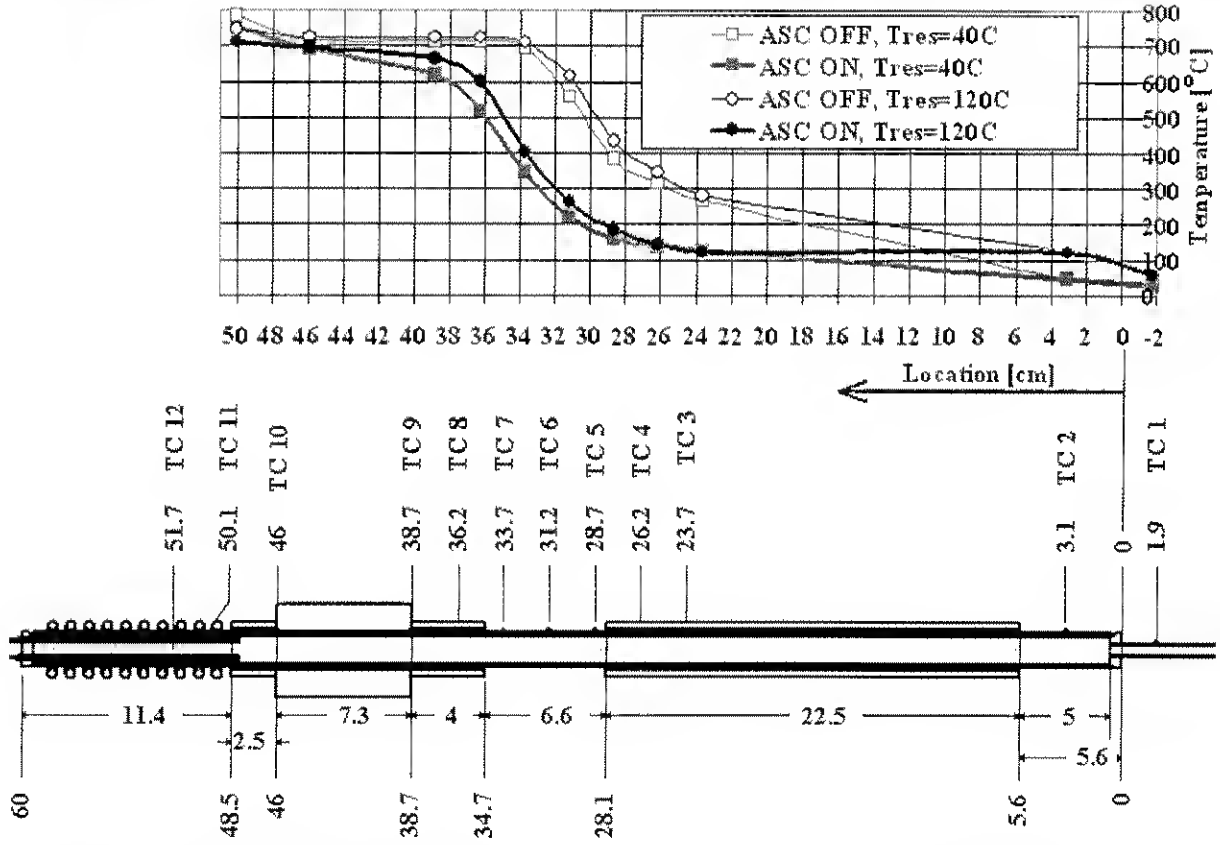

FIGURE 9. VCHP Experimental Results, Showing the Ability of the VCHP to Turn On When the Stirling Convertor is Off.

CONCLUSIONS

Previous VCHPs were designed to maintain the heat pipe temperature near a fixed point, as the power varies. In contrast, the current VCHPs were designed to operate with a radiator that is either all on, or all off. The program demonstrated the feasibility of using a VCHP for backup cooling of the GPHS to allow the Stirling convertor to be

stopped and restarted: (1) The VCHP turns on with a ΔT of 30 °C, which is high enough to not risk standard ASRG operation but low enough to save most heater head life, (2) A low mass design was developed that integrates with the ASRG, and (3) thermal losses are reasonably low for normal operation and can be further reduced. Additional benefits of the VCHP are reduced GPHS surface temperature, and a more isothermal heater head.

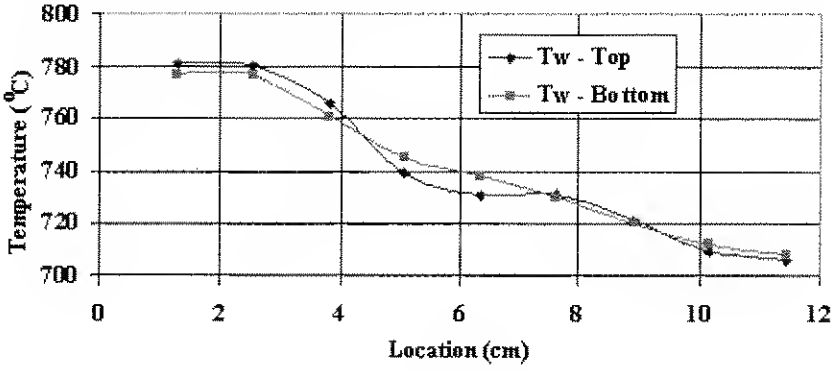

FIGURE 10. Evaporator Temperature Profile, Showing the Effects of the Change in Composition.

In addition to the successful design, a proof-of-concept NaK VCHP was fabricated and tested. While NaK is normally not used in heat pipes, it has an advantage in that it is liquid at the reservoir operating temperature, while Na or K alone would freeze. The VCHP had two condensers, one simulating the heater head, and the other simulating the radiator. The experiments successfully demonstrated operation with the simulated heater head condenser off and on, while allowing the reservoir temperature to vary over 40 to 120 °C, the maximum range expected. In agreement with previous NaK heat pipe tests, the evaporator ΔT was roughly 70°C, due to distillation of the NaK in the evaporator. This should be reduced in the ASRG VCHP.

ACKNOWLEDGMENTS

This research was sponsored by NASA Glenn Research Center under Contract No. NNC07QA40P. Lanny Thieme was the technical monitor. We would like to thank Jeff Schreiber and Jim Sanzi of NASA Glenn Research Center, and Jack Chan of Lockheed Martin Space Systems Company for helpful discussions about the Stirling system and the VCHP. We would like to thank Roy Tew of NASA Glenn Research Center for running cases with the Sage Stirling thermodynamic code to estimate the effects of isothermalizing the heater head with the VCHP. Rod McClellan was the technician for the program.

REFERENCES

Anderson, W. G., Rosenfeld, J. H., and Noble, J., "Alkali Metal Pool Boiler Life Tests for a 25 kWe Advanced Stirling Conversion System," *Proceedings of the 26th Annual IECEC*, D. L. Black, ed., **Vol. 5**, pp. 343-348, American Nuclear Society, LaGrange Park, IL, 1991.

Anderson, W. G., "Sodium-Potassium (NaK) Heat Pipe," *Heat Pipes and Capillary Pumped Loops*, Ed. A Faghri, A. J. Juhasz, and T. Mahefky, ASME HTD, 236, pp. 47-53, 29th National Heat Transfer Conference, Atlanta, Georgia, August 1993.

Andraka, C. E., Goods, S.H., Bradshaw, R.W., Moreno, J.B., Moss, T.A. and Jones, S.A., "NaK Pool-Boiler Bench-Scale Receiver Durability Test: Test Results And Materials Analysis," *Proceedings of the 29th IECEC*, **Vol. 4**, pp. 1942-1949, AIAA, Washington, D.C., 1994.

Chan, T.S., Wood, J. G. and Schreiber, J. G., "Development of Advanced Stirling Radioisotope Generator for Space Exploration," NASA Glenn Technical Memorandum NASA/TM-2007-214806, 2007.

Crockfield, R.D. and Chan, T.S., "Stirling Radioisotope Generator for Mars Surface and Deep Space Missions," *Proceedings of 37th IECEC*, **Vol. 1**, pp. 134-139, IEEE, Washington, D.C., 2002.

Ernst, D. M., Advanced Cooling Technologies, Inc, personal communication, 2007.

Marcus, B. D., "Theory and Design of Variable Conductance Heat Pipes," NASA Report NASA-CR-2018, April, 1972.

Rosenfeld, J. H., Ernst, D. M., Lindemuth, J. E., Sanzi, J., Geng, S. M., and Zuo, J., "An Overview of Long Duration Sodium Heat Pipe Tests," NASA Glenn Technical Memorandum NASA/TM—2004-212959, 2004

Tew, R., NASA Glenn Research Center, personal communication, 2007.